ISSN No: -2456-2165 https://doi.org/10.38124/ijisrt/26apr2362

Investigation on the Heat Exchanger with Passive Techniques for the Enhancement of Heat Transfer

Hemavathi P.[1]; Vijaya Kumar Reddy K.[2]

[1,2]Department of Mechanical Engineering, JNTUH College of Engineering, Hyderabad

Publication Date: 2026/05/16

Abstract: In the current decade, heat exchangers play an important role in optimizing energy utilization, improving HVCE performance, and reducing carbon emissions in a variety of sectors. Shell and tube heat are frequently utilized to achieve this. Using a 40° helical baffle in the shell side and twist tape in the tube, the shell and tube heat exchanger is studied numerically to enhance heat transmission. The investigation is carried out using twisted tape inserts with pitches of 50, 100, 150, and 200 mm, as well as varied mass flow rates. The results display flow and thermal parameters, including pressure drop, friction factor, heat transfer coefficient, Nusselt number, and thermal performance. When compared to the traditional design, the Nu increases by 10.84%, 17.55%, 23.52%, and 31.21% as the twist tape pitch increases. The creation of swirl flow in the tube causes the fluid to mix well. Also, when the mass flow rate and twist pitch length rise, the factor of friction decreases. The rate of increase in friction factor is 70.81%, 47.04%, 37.43%, and 31.34% for twist pitches of 50, 100, 150, and 200 mm. However, the performance evaluation criterion (PEC) reveals that best thermo-hydraulic performance is reached at a twist tape pitch of 150 mm, which is 19.60% higher than the other values. It is shown that using helical baffles in conjunction with twisted tape inserts is a great and useful way to improve heat exchanger thermal efficiency.

Keywords: *Shell-and-Tube Heat Exchanger; Twisted Tape Inserts; Helical Baffles; Heat Transfer Enhancement; Pressure Drop; PEC.*

How to Cite: Hemavathi P.; Vijaya Kumar Reddy K. (2026) Investigation on the Heat Exchanger with Passive Techniques for the Enhancement of Heat Transfer. *International Journal of Innovative Science and Research Technology*, 11(4), 4764-4777. https://doi.org/10.38124/ijisrt/26apr2362

I. INTRODUCTION

In this decade, heat exchangers have helped numerous sectors reduce carbon emissions, boost performance, and optimize energy use. Waste heat recovery is essential for many industrial applications. Sustainability ideals are supported by heat recycling's significant carbon footprint and energy savings. Heat exchanger technology advances via efficiency, sustainability, lifespan, and cost optimization. These improvements are necessary for modern industrial applications and provide a long-term energy and environmental answer. Food, dairy, chemicals, pharmaceuticals, and pulp & paper sectors use heat exchangers to maintain product quality and temperature. Businesses may lessen their environmental effect without compromising productivity by adopting these technologies. Heat exchanger technology may boost efficiency and lifespan, helping businesses balance profitability and sustainability. Demand is often met by shell-and-tube heat exchangers (STHXs). STHX thermal performance must be improved to decrease energy consumption, operational costs, and environmental impact.

Passive heat transfer augmentation methods are popular due to their simplicity and cheap maintenance. Twisted tape promotes turbulence and swirl flow in tube walls, improving heat transfer. Heat transfer improvement increases pressure drop; therefore, hydraulic performance must be balanced. Helical shell-side baffles increase heat transfer over segmental baffles by facilitating continuous crossflow and decreasing flow stagnation. Twisted tape inserts or helical baffles increase STHX thermohydraulic performance. Researchers considered many STHXs improvements.

Baffle geometry was employed to investigate STHX thermal performance. Chen et al. [2025] [1] statistically analysed helical baffle heat exchangers that use elliptical and circular tubes to transfer heat and flow molten salt nanofluid. Elliptic tubes reduce shell-side pressure loss by 43.45% and increase heat transmission by 5.45%-8.51%. Elliptic tubes provide 1.85 times greater transfer of heat per unit pressure drop. Its average TPF is 1.39, indicating efficiency. Future molten salt heat exchangers can use these discoveries to improve thermal and flow performance. Dinesh Babu et al. [2024] [2] examined thermo-hydraulic performance of standard shell-and-tube heat exchangers (STHE) with single/double segmental, helical, NTIW, propeller, and spiral baffles. HTRI and CFD analysis were used. LMTD, NTU, total heat transfer coefficient, efficacy,

ISSN No: -2456-2165 https://doi.org/10.38124/ijisrt/26apr2362

and exergy efficiency were measured at constant flow and temperature. All indicators benefit from double segmental and single helical (15°) baffles. With these data, more efficient baffle designs may be chosen. Saad et al. [2023] [3] created a shell-and-tube heat exchanger (STHX) with trefoil holes in segmental baffles. STBs were compared to segmental (SGB) and trefoil hole baffles (THB) using ANSYS FLUENT simulations at varying flow rates. Although STBs and SGBs both transport heat, STBs have less dead and recirculation zones and pressure drops. With baffles, thermohydraulic performance rose by 41% over SGBs and 235% over THBs, reaching 57%. STBs outperformed conventional designs regardless of clearance. Gugulothu et al. [2022] [4] conducted a CFD study on a shell-and-tube heat exchanger (STHX) employing Al_2O_t, CuO, and SiO_2 nanofluids at concentrations from 1 to 5 vol.%. The hot STHX heated water, while the cold side employed nanofluids. Nanofluid concentration increases heat transfer coefficients for Al_2O_3, SiO_2, and CuO by 10.41%, 9.56% and 12.27% at 5 vol.% and 0.22 kg/s. Nanofluids lower pressure further. The research found that nanofluids increase STHX performance while fulfilling TEMA criteria. Cao et al. [2025] [5] performed numerical calculations on a Y-type spiral baffle design to address the triangle leakage zone inside the Quarter Helical Baffle heat exchangers. To improve performance, the Response Surface Methodology was used to change the axial angle tilt (α) to 25°, circumferential angle tilt (β) to 35°, and overlap ratio (δ) to 5 mm. Increased overlap ratio reduced leakage and improved vortex and heat transmission. The most significant factor was the axial angle α, especially when paired with β. The modified Y-type design increased industrial heat recovery efficiency by 25-40% by improving heat transport.

Cheng et al. [6] say helical baffle heat exchangers (HBHEs) are intensively explored because they exceed shell-and-tube heat exchangers in thermal performance and flow resistance. Helical baffle design, pitch, and shell-side flow patterns have been improved to reduce pressure drop and increase heat transmission. Nusselt number, heat transfer coefficient, and friction factor have been used in many computational and experimental performance studies. The design innovations industry uses CFD analysis and optimization extensively. Managing heat transfer and pressure loss during manufacturing remains difficult. Shuai et al. modelled a discontinuous helical baffle heat exchanger for power plant steam condensation waste heat recovery [2025] [7]. Shell-side condensation and steam input cooling water temperature, velocity, and flow are investigated using ANSYS Fluent 2020R1. As steam input velocity increases from 5 to 20 m/s, the shell-side heat transfer coefficient climbs 81.22%, but as steam superheat decreases from 10 to 50 K, it lowers 16.69%. This research confirms the exchanger works and suggests ways to enhance industrial condensation systems. Lu et al. [2024] [8] developed a grooved helical baffle design that improves quadrant heat exchanger structural stability and performance. Both the shell and tube sides of FLUENT 2017 numerical simulations used liquid water. Overlapping baffles and helical angles altered heat transmission and flow. Performance is optimal with a 50° helix angle and 0.5 overlap. Heat transmission improves with reduced flow resistance. Regression analysis yielded a shell-side heat transfer coefficient correlation formula. The article provides industrial grooved helical baffle heat exchanger design advice. Cheng et al. [2024] [9] modelled a helical baffle heat exchanger with corrugated tubes. Passive improvement increases energy efficiency with little operating complexity. The heat transfer coefficient rises by 20% when the helix angle is reduced from 28.42° to 10.81°. Efficiency evaluation coefficient (EEC) measures performance. The optimum structural characteristics for different operating circumstances dictate heat exchanger design. Vivek et al. [2024] [10] built a helix changer model to study how water and calcium chloride brine mass flow rates (MFR) affect heat transfer coefficient (OHTC). Both fluids' OHTC rises with MFR, but brine, being warmer, plateaus. As cold fluid MFR develops, shell-side pressure reduction increases. These studies demonstrate the relevance of flow rate in hydraulic and thermal performance in airplane and vehicle high-pressure systems. Kaleru et al. [2022] [11] examined a TEMA shell-and-tube heat exchanger (STHX). The heated fluid was water; the cold fluid was another. Helical and segmental baffles (HBs and SBs) at 20, 30, 40, and 50 degrees of inclination were numerically and experimentally evaluated. SBs' higher Colburn factor (j_s) implied better heat transmission. The 40° angled HB arrangement offered the lowest shell-side pressure drop for heat transfer and flow resistance.

Hu et al. [2023] [12] used SolidWorks 3D models and ANSYS simulations to study how baffle design and type affect shell-and-tube heat exchanger (STHX) thermo-hydraulic performance. We analyse the pressure drop, heat transfer coefficient, and isobaric JFP factor of the shell. Segmental baffles should have 200 mm spacing, 0.4 mm gap height, and 150 mm pitch. Helical baffle STHX outperformed segmental baffle STHX by 1.18 times in JFP factor. Gu et al. [2023] [13] suggested replacing flat baffles (FB) with sinusoidally corrugated ones to improve torsional flow heat exchangers (TFHXs) thermal performance. Shell-side flow resistance and heat transmission are modelled by full-section CFD. SCBs increase baffle flow homogeneity and turbulence. The ideal SCB parameters are discovered using CCD-RSM: amplitude = 1.37 mm, cycles = 4.42, and beginning phase = 112.73°. The heat transfer coefficient increases 11.58% and performance increases 5.48% under these conditions. LDV experiments verify simulation accuracy. This should optimise TFHX structure. A hybrid nanofluid of alumina, copper, and water was used to quantitatively assess a shell and tube heat exchanger (NCHB-STHX) with non-continuous helical baffles at different concentrations and flow rates by Jalili et al. [2022] [14]. They model helix angles from 20° to 40° with Reynolds values from 25,000 to 31,000. The K-ε RNG model was deemed most appropriate. At 20 degrees, the helix angle increases heat transmission while 40 degrees decreases pressure reduction. Heat transfer increased by 84% and HTC/ΔP improved by 6% using a 2% hybrid nanofluid at 1.685 kg/s at 20°, compared to previous experiments. Marzouk et al. [2022] [15] evaluated CSS, SSS, FS, HS, CR, and CRH baffle designs using shell and tube heat exchanger computer modelling. The thermal and

ISSN No: -2456-2165 https://doi.org/10.38124/ijisrt/26apr2362

hydraulic performance investigation focused on effectiveness (ε), heat transfer coefficient (h), and pressure loss from 10,500 to 38,500 Reynolds numbers. Both the HS and CR designs improve thermal performance, however the HS has the most pressure drop. FS and HS reduce dead zones whereas CRH eliminates them. CRH is superior because it has 166% greater efficiency and 142% higher heat transfer coefficient than CSS. Friction losses are much smaller than HS and CR. A 138% better heat transfer coefficient per pressure loss, CRH beats all other designs. Chen et al. [2021] [16] statistically investigated shell-side thermal and overall performance of a new latent heat exchanger with sextant helical baffles at 10°-40° helix angles. Adjusting internal-external fin height, thickness, and form increases phase change material (PCM) melting. 7.5 mm tall, 1 mm thick longitudinal fins work well. Results demonstrate that hydraulic oil, water, ethylene glycol, and JP-4 fuel oil perform better with higher thermal conductivity and lower Prandtl values. We examine nano-PCM discharge behaviour with varying TiO_2 concentrations (2%, 4%, 6%). The results show that the helix angle and Nano-PCM must balance thermal conductivity and latent heat. The work improves latent heat thermal energy storage devices. Uosofvand et al. [2021] [17] used SolidWorks Flow Simulation to simulate a hybrid segmental-helical baffle shell-and-tube heat exchanger (HSHB-STHX). Ribbed tubes with circular, triangular, or rectangular ribs with a hybrid baffle system in a single shell pass improve thermal performance. Hydrothermal efficiency, pressure drop, and other parameters are assessed. The most effective arrangement is HSHB-STHX, with six segmental baffles, a right angle, and ribbed rectangular tubes. This design improved PEC by 41%, HSHB-STHX without ribs by 35.54%, and segmental baffle by 37%. Heat transfer improves with a rectangular ribbed tube and controllable pressure loss. Performance is compared to identify the best baffle and rib shape. The findings provide efficient commercial heat exchanger design suggestions. Gugulothu et al. [2021] [18] revised designer parameters for shell and tube heat exchangers (STHEs), which are commonly used in industry, to simplify and enhance efficiency. Previous study suggested an optimal 40° helical baffle STHE. RSM models and analyses system performance under diverse conditions. Design Expert program finds optimal design variables. Each solution improves system performance, proving the statistical model for STHE design optimization works.

Wang et al. [2021] [19] examined the thermal-hydraulic performance of a branch baffle heat exchanger with shell-side oblique and local jet patterns. CFD programs ran fluid dynamics, temperature, and pressure models and verified them with Laser Doppler Velocimetry. Branch baffles reduce pressure loss and heat transfer coefficient better than segmental and shutter baffles at identical flow rates. Comparing segmental and shutter baffle efficiency assessment criteria, we find 28–31% and 13.2%–14.1% increases, respectively. The field synergy analysis suggests a more energy-efficient heat exchanger design with greater velocity and pressure gradient coordination. Cao et al. [2020] [20] studied fluid flow and heat transfer in shell-and-tube heat exchangers using eight helical baffle designs, including a continuous (CH), quadrant (QH) with varying axial overlaps, and unique sextant (SH) design. Experimental validations match CFD models. The second law of thermodynamics calculates entropy and irreversibility. We study leakage via baffle notches and offer the swirl angle to define the shell-side stream pattern to identify spiral and pseudo-spiral flow. The results show that baffle form and construction greatly impact flow. SH outperforms CH and QH thermo-hydraulically. SH and QH yield the least entropy at low Reynolds numbers. With increased axial overlap ratios, heat transport and pressure drop improve while performance ratios and thermodynamic losses decrease. This extensive investigation shows that SH can replace baffles. Abdelkader et al. [2020] [21] predicted shell-and-tube heat exchanger performance using EES software. The model uses Bell-Delaware for segmental baffles and mathematical correlations for helical baffles. It matches published experiments. Helical baffles outperform segmental ones thermally. Helical baffle performance depends on baffle angle. Performance drops at 42 degrees of baffle angle. The ideal helical baffle angles result. The model simplifies shell-and-tube heat exchanger design with changeable baffles. Engineers can use it to improve industrial heat exchangers. Twist tape on the tube side blocked fluid flow to increase heat exchanger performance. In turbulent flow conditions, Anbu et al. [2025] [22] extensively studied the impact of HCTs, SRIs, and Al_2O_3-water nanofluids on convective heat transfer. Height, insert pitch, nanoparticle volume concentration (0.25% and 0.5%), and corrugation pitch affected Nusselt number and friction factor. Nanofluids alone increased the Nusselt number in a smooth tube by 15.2% over water. Low-pitch inserts with 0.5% nanofluid and high-corrugation-height, low-pitch increased Nu by 83.43% and friction factor by 81.1%. Internal inserts, nanofluids, and surface shape changes can improve current heat exchanger thermal performance. Marzouk et al. [2024][23] compared segmental baffles with spring wire inlays to improve heat transmission in shell and multi-tube heat exchangers. In the Reynolds number range of 8500-12500, the study examined the impacts of experimental and computational methods on Nusselt number, pressure drop, and exergy efficiency. In the basic tube enclosure, spring wires enhanced heat transmission 1.61 times and baffles 1.54 times. Both methods increased pressure drop, but spring inserts accounted for 87% of the baffle's pressure drop, increasing the pressure-to-performance ratio. Spring wire designs improved exergy efficiency. The investigation found that SMTHX spring inserts perform better thermally and hydraulically than baffles.

Louahdi et al. [2024] [24] three-dimensional numerical analysis enhanced heat exchangers with perforated semi-circular inserts' thermo-hydrodynamic performance. Given the worldwide energy crisis, the research sought to improve industrial waste heat recovery by developing more compact and efficient heat exchangers. Multiple working fluid combinations and inserts were used to assess thermal performance throughout a wide Reynolds number range. Model 2, with perforations, has the greatest thermal performance factor among the five geometries at 140,000

ISSN No: -2456-2165 https://doi.org/10.38124/ijisrt/26apr2362

Reynolds number, 1.8787. Perforated semicircular inserts increase turbulence and mixing and reduce pressure losses by evenly distributing flow, according to research. The results show that heat exchangers may balance thermal and hydraulic performance with geometrically optimized inserts. This may benefit energy-intensive firms. Deshmukh and Sarviya [2024] [25] grouped experimental and computational studies on twist tape (TT) inserted in single-phase flow tubular heat exchangers. The research recommends passive augmentation methods, notably twisted tape inserts, for their simplicity, affordability, and retrofit ability. Twist tape designs might be clockwise, anticlockwise, alternating, or hybrid patterns with twisted and untwisted components, according to the assessment. This research details heat transmission and pressure drop consequences for each design. It statistically analyses Nusselt numbers and friction factors to assess swirl flow insert and baseline smooth tube thermal-hydraulic performance. To be viable, twist tape inserts need a TPF above 1.0. Geometry optimization and hybrid enhancement research should focus on application-specific cost and performance parameters, the authors advise. Marzouk et al. [2023][26] investigated a complete and current heat transmission improvement set for shell-and-tube heat exchangers. Heat transfer coefficient (U), number of transfer units (NTU), energy efficiency, pressure drop, and thermal-hydraulic performance were used for method classification and evaluation. Chemical procedures make up 9.7% of this study's broad classification of augmentation methods, air injection 20.2%, nanofluids 22.3%, and passive methods 47.8%. The U ratio rose 452% over water-only flows with air bubble injection, 130% with swirl vanes, 161% with corrugated tubes, and 264% with wire coil inserts. The highest thermal performance enhancement (175.9% U ratio) was seen in TiO_2 nanofluids. The experts recommended air infusion with passive inserts for compound enhancement due to its synergistic benefits. The literature lacks theoretical studies and numerical simulations, therefore future recommendations should focus on geometrical optimization, coating techniques, and empirical correlations backed by additional numerical simulations.

Kaushik et al. [2023][27] examined a cascaded spiral copper tube heat exchanger with conical, hemispherical, and helical inserts for thermo-hydraulic performance under turbulent counter-flow conditions utilizing water. Experiments employed water temperatures from 304 K to 333 K and Reynolds numbers from 4236 to 18,545. Helical, conical, and hemispherical inserts outperformed simple spiral tubes by 18.5%, 15.5%, and 11.5%, respectively. The key performance measures included heat transfer rate, Nusselt number, friction factor, effectiveness, NTU, and thermal performance factor (ηtp). Using a 2 mm diameter, 10 mm pitch helical insert, the highest value of 1.51 was attained at 13,322 Reynolds number, with ηtp ranging from 1.24 to 2.51. Helical inserts are best for spiral tube heat exchangers thermally and flow-wise, according to this study. Ifraj et al. [2023][28] used numerical analysis to maximize thermal efficiency of a heat exchanger tube with Y-shaped metallic inserts and hybrid, hexagonal, trapezoidal, or kite-shaped holes. Air was employed at 3000–21000 Reynolds numbers, and the perforation index (PI) was 10%–30%. The trapezoidal perforation with PI = 20% had the highest thermal performance factor (TPF) of 3.68, 225 Nusselt numbers at Re = 21000, and the lowest friction factor (f = 0.07). However, hexagonal perforations at PI = 10% had the greatest friction factor (f = 0.24) and increased flow resistance. Compared to a smooth tube, Nusselt number rose 6.15 and friction factor 5.03. According to the investigation, the trapezoidal PI 20% insert performed best, and insert geometry and perforation design effect heat transfer enhancement and pressure decrease. Tavousi et al. [2023][29] critically reviewed how to improve passive heat transfer in twin tube heat exchangers. DTHEs are appropriate for the study's focus on producing cost-effective heat exchangers with high heat transfer rates and low pressure drop because to their simplicity and extensive industrial use. Besides active methods, the review examined turbulator inserts, hybrids, changed tube geometry, extended surfaces (fins), and nanofluids. Heat transfer and friction factor increases were statistically compared for each approach. In a standard deviation investigation, turbulator inserts and nanofluids had the maximum heat transfer enhancement potential, whereas extended surface approaches (fins) performed poorly due to their high friction factor. The research recommends studying chemical enhancement and optimum geometrical designs in DTHEs and identifies knowledge gaps.

In 2021, Toygun et al. [30] reported... An experiment examined how twisted tape inserts improve turbulent flow heat transfer. Tape edges contained dimples and perforations, and twist ratio was 5.88. Compared to smooth tubes, all twisted tape inserts increased thermal performance. Dimples transmitted heat better than perforated tapes, which reduced friction. Twisted tape had the greatest PEC at 1.57 with a dimple pitch ratio of 0.25. Marzouk et al. 2022[31] provided this information. Tube inserts were tested to improve shell-and-tube heat exchanger heat transmission. Tubes had 10 cm and 5 cm inserts. The study used one, two, and three litters per minute air volumetric flow rates. Studying thermal and hydraulic characteristics. A 5 cm space between inserts increases flow disruption and mixing, improving thermal performance. A 2020 review by Pongjet et al. [32]. Theoretical-experimental research used discrete V-winglet (DW) tapes in V-up and V-down configurations to improve tubular heat exchanger heat transmission. At 30° angle of attack, this study studied the effects of four relative pitches (Rp = P/D = 0.5, 1.0, 1.5, and 2.0) and three relative winglet heights (RB = b/D = 0.1, 0.15, and 0.2). The shortest pitch length (Rp = 0.5) gave the highest Nusselt number and friction factor at all winglet heights. In the RB = 0.2 and Rp = 0.5 arrangement, friction factor increased 18.8 times and heat transfer (Nusselt number) 3.8 times. The design with 1.0 pitch and 0.15 winglet height has the greatest Thermal Performance Enhancement Factor with V-up of 1.99 and V-down of 2.02. V-winglet tape inserts, especially V-down ones, may improve heat exchanger thermal performance. Source: Suabsakul et al. 2020[33]. Experimentally, wavy fin inserts with 0.5, 1.0, and 1.5 amplitude-to-height ratios increased tube heat transfer. The Nusselt number ratio increased 8%

ISSN No: -2456-2165 https://doi.org/10.38124/ijisrt/26apr2362

and 16% over the plain tube for A/h values of 1.0 and 0.5. At lower Reynolds numbers, heat transfer enhancement performance peaked with a performance enhancement factor of 1.51 and an area/hour ratio of 1.5. At low flow rates, the A/h ratio enhances the thermal performance benefits of wavy fin inserts.

This study investigates the combined effects of helical baffles on the shell side of a STHX and twisted tape inserts on the tube side. A detailed investigation is conducted into the impact of twisted tape pitch on heat transfer characteristics, pressure drop, friction factor, and overall performance evaluation criterion. Unlike prior research, which examined either twisted tape inserts or helical baffles separately, the current study statistically evaluates their combined thermo-hydraulic impact in a shell-and-tube heat exchanger with optimal twist pitch. The study also discovers an ideal pitch using PEC analysis under regulated operating circumstances.

II. NUMERICAL METHODOLOGY

The numerical study is carried out on STHXs at different mass flow rates of working fluid. Helical baffles are placed at a 40-degree angle on the shell side, while twist tapes are put on the tube side. The numerical analysis is carried out using ANSYS R24/25, with appropriate boundary conditions.

- *Heat Exchanger Configuration*

The STHXs have a single shell-pass and a single tube-pass at the shell and tube of the heat exchanger, respectively. A cylindrical shell has four bundles of circular tubes. Twisted tape inserts are put within the tubes to improve tube-side heat transmission, while helical baffles angled at 40° are attached on the shell side to encourage crossflow and equal fluid distribution. The exterior diameters of the tube and shell are 25.40 mm and 109.94 mm, respectively. The inner diameters of HX tubes and shells are 20.32mm and 101.10mm, respectively. The pitch is specified as 31.75 mm. The hydraulic diameter is measured at 25.13mm as shown in the figure 1.

- *Twisted Tape Inserts*

Twisted tape inserts with pitches of 50, 100, 150, and 200 mm developed and inserted into the tubes. The variation in pitch allows for controlled modification of swirl intensity and turbulence generation within the tube-side flow as shown in the figure 2 and 3.

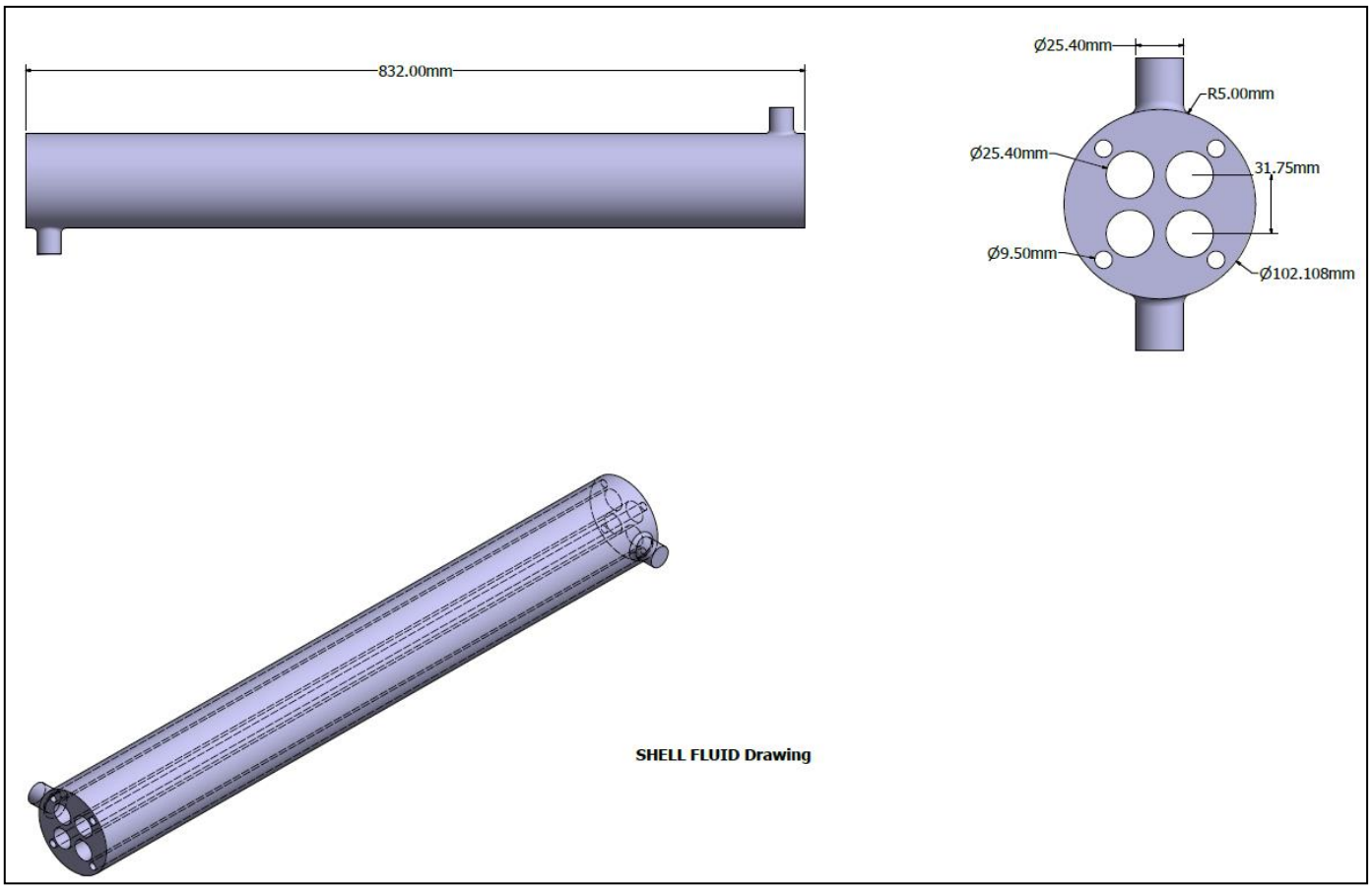

ISSN No: -2456-2165 https://doi.org/10.38124/ijisrt/26apr2362

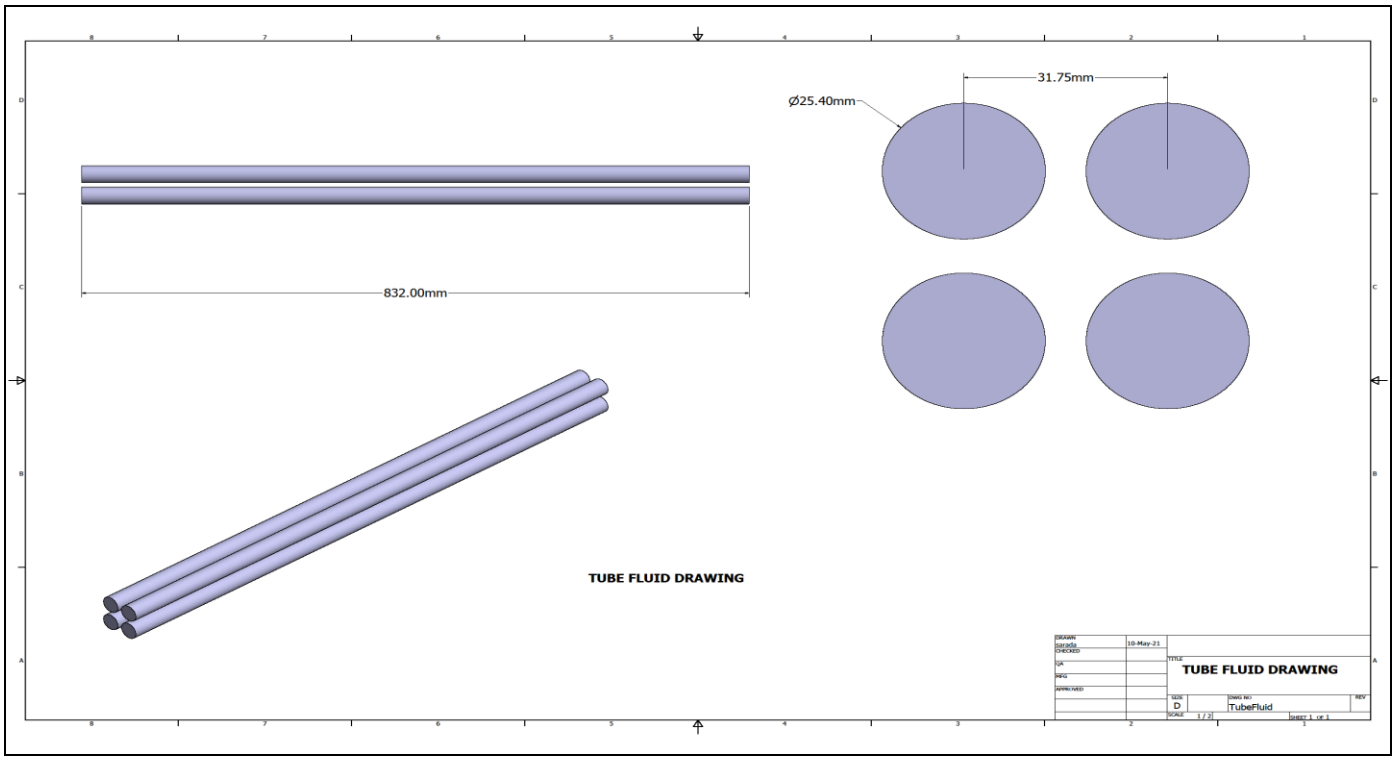

Fig 1 Geometry of Shell and Tube Heat Exchanger

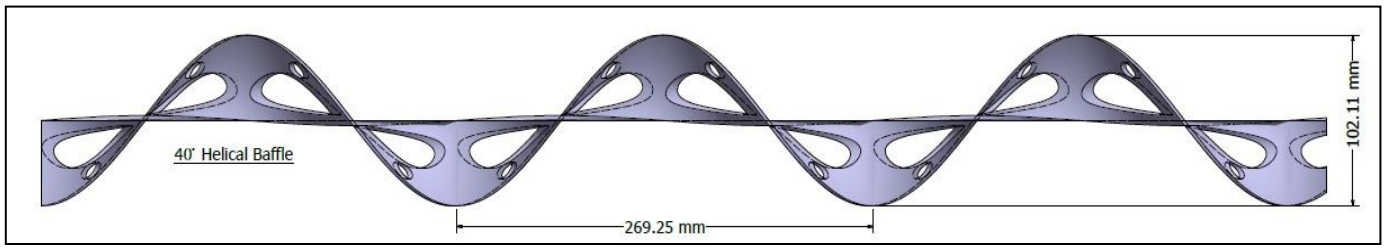

Fig 2 Helical Baffles with an Angle of 40°

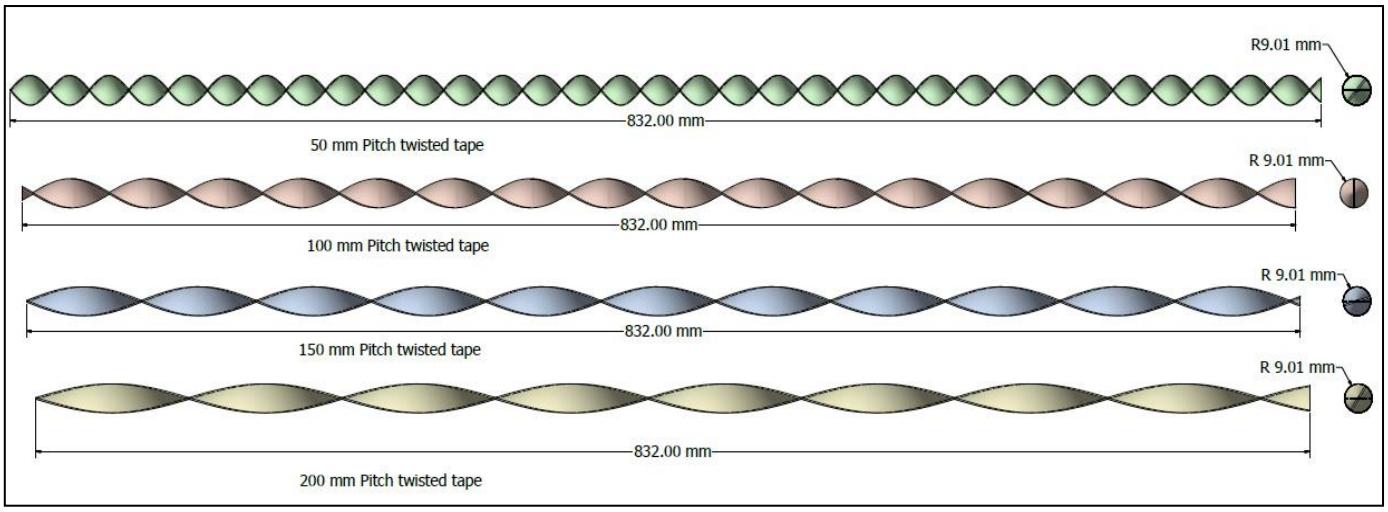

Fig 3 Twist Tape Inserts with Various Pitches

➢ *Generation of Mesh and Gird Independence Test*

The mesh is constructed with different element sizes to forecast the accurate solution in mesh modular. The element size varies from m to m (nodes range from 0.5 million to 3.28 million). At 3.28 million nodes, the cold and hot outlet temperatures stabilized. As a result, after analysing the grids and taking the results into consideration, 3.28 million nodes with element sizes of 0.001 m are regarded optimum grids, and future simulations are performed using that grid system. The average orthogonal quality is 0.83, skewness is 0.22, and aspect ratio is 2.62 as shown in the figure 4.

ISSN No: -2456-2165 https://doi.org/10.38124/ijisrt/26apr2362

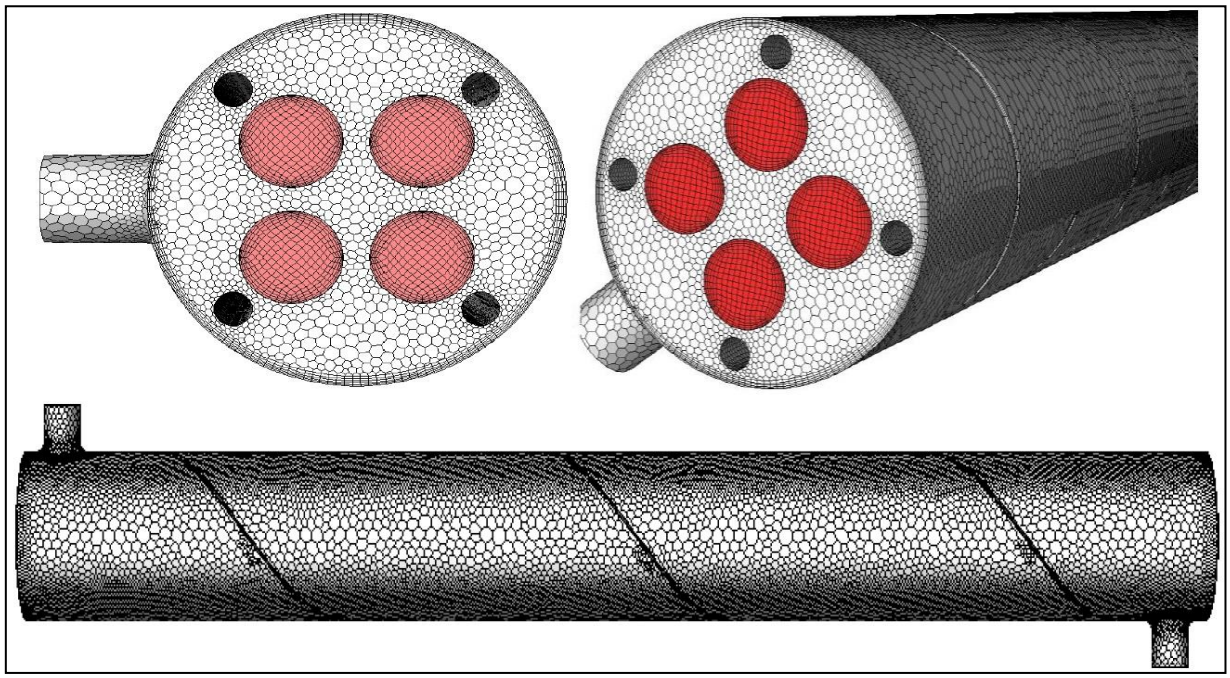

Fig 4 Mesh generated for STHXs

➢ *Governing Equations*

The simulation model utilizes k-ε turbulence models to provide accurate and optimal results. It enhances wall flow, vortex production, fluid rotation, and so forth. This analysis takes into account both steady-state heat transfer and turbulent in-compressible fluid flows. The governing equations are as follows, solved with boundary conditions [34]:

Law of Conservation of Mass: $$\frac{\partial(\rho u_i)}{\partial x_i} = 0 \quad (1)$$

Navier-Stokes equations: $$\frac{\partial(\rho u_i u_k)}{\partial x_i} + \frac{\partial p}{\partial x_k} = \frac{\partial\left(\mu \frac{\partial u_k}{\partial x_i}\right)}{\partial x_k} \quad (2)$$

Steady flow energy equation: $$\frac{\partial(\rho u_i t)}{\partial x_i} = \frac{\partial\left(\frac{k}{C_p}\frac{\partial t}{\partial x_i}\right)}{\partial x_i} \quad (3)$$

Transport equation: $$\frac{\partial(\rho k)}{\partial t} + \frac{\partial(\rho k u_i)}{\partial x_i} = \frac{\partial\left(\frac{\alpha_k \mu_{eff} \partial k}{\partial x_j}\right)}{\partial x_j} + G_k + \rho\varepsilon \quad (4)$$

Transport equation for dissipation: $$\frac{\partial(\rho\varepsilon)}{\partial t} + \frac{\partial(\rho\varepsilon u_i)}{\partial x_i} = \frac{\partial\left(\frac{\alpha\varepsilon\mu_{eff}\partial\varepsilon}{\partial x_j}\right)}{\partial x_j} + \frac{G_k \varepsilon C_{1\varepsilon}^*}{k} - \frac{C_{2\varepsilon}\varepsilon^2\rho}{k} \quad (5)$$

ISSN No: -2456-2165 https://doi.org/10.38124/ijisrt/26apr2362

Where,

$$\mu_{eff} = \mu + \mu_t,\ \mu_t = \rho\frac{k^2}{\varepsilon}c_\mu,\ C_{1\varepsilon}^* = C_{1\varepsilon} - \frac{\eta\left(1-\frac{\eta}{\eta_0}\right)}{1+\beta\eta^3},\ \eta = \frac{k}{\varepsilon}\left(E_{ij}2E_{ij}\right)^{0.5},\ E_{ij} = \frac{1}{2}\left[\frac{\partial u_i}{\partial x_j} + \frac{\partial u_j}{\partial x_i}\right]$$

The observed empirical values are as follows [26][35][36]:

$$C_\mu = \frac{845}{10{,}000},\ C_{1\varepsilon} = \frac{142}{100},\ C_{2\varepsilon} = \frac{168}{100},\ \beta = \frac{12}{1000},\ \eta_0 = \frac{438}{100},\ \alpha_\varepsilon = \alpha_k = \frac{139}{100}$$

Volume flow rate in Shell side = $\frac{\text{liter per minute}}{60*1000}\ \frac{m^3}{s}$ (6)

Mass flow rate at Shell side $\left(\frac{kg}{s}\right)$ = volume flow rate $\left(\frac{m^3}{s}\right)$ * Density (ρ_s) $\left(\frac{kg}{m^3}\right)$ (7)

velocity of fluid in shell side [70] $V_s = \frac{\dot{m}_s}{\rho_s A_s}\frac{m}{s}$ (8)

heat capacity rate at Shell side [187] $C_h = m_h C_{p,h}$ (9)

Tube side volume flow rate= $\frac{\text{liter per minute}}{60*1000}\ \frac{m^3}{s}$ (10)

Tube side mass flow rate $\left(\frac{kg}{s}\right)$ = volume flow rate $\left(\frac{m^3}{s}\right)$ × Density (ρ_t) $\left(\frac{kg}{m^3}\right)$ (11)

Heat capacity rate can be expressed as [37] $C_c = m_c C_{p,c}$ (12)

Capacity ratio [113] $C^* = \frac{\left(mC_p\right)_{\min}}{\left(mC_p\right)_{\max}}$ (13)

NTU is [113][187] $NTU = \frac{UA_0}{\left(mC_p\right)_{\min}}$ (14)

$$\varepsilon = \frac{1-e^{-NTU\left(1-C^*\right)}}{1-C^*e^{-NTU\left(1-C^*\right)}} \quad (15)$$

Heat exchanger effectiveness expressed as follows:

$$\varepsilon = \frac{2}{\left[1+C^*+\sqrt{1+C^{*2}}\times\frac{1+e^{-NTU\sqrt{1+C^{*2}}}}{1-e^{-NTU\sqrt{1+C^{*2}}}}\right]} \quad (16)$$

ISSN No: -2456-2165 https://doi.org/10.38124/ijisrt/26apr2362

To calculate unknown parameter $\varepsilon = \frac{(mC_p)_{\min}}{T_{h,i} - T_{c,i}} = \frac{T_{c,2} - T_{c,i}}{T_{h,i} - T_{c,i}}$ (17)

Cold fluid outlet temperature $T_{c,o} = T_{c,i} + \varepsilon(T_{h,i} - T_{c,i})$ (18)

The outlet temperature of hot fluid is $T_{h,o} = T_{h,i} - \left(\frac{(mC_p)_c}{(mC_p)_h} \times (T_{c,o} - T_{c,i}) \right)$ (19)

Hot fluid bulk temperature [38][39] $T_{h,b} = \frac{T_{h,i} + T_{h,o}}{2}$ (20)

Cold fluid bulk temperature [38][39] $T_{c,b} = \frac{T_{c,i} + T_{c,o}}{2}$ (21)

➢ *Boundary Condition:*

Tube side flow rate varied from 0.23 to 0.43 kilogram per second. Shell side flow rates are litres per minute are taken and overall heat transfer coefficient is assumed as 1000.

- Shell side fluid (hot) temperature $(T_{h,i}) = 70^0 C = 343.15K$
- Tube side fluid (cold) temperature $(T_{c,i}) = 28^0 C = 301.15K$
- Shell side: hot fluid
- Tube side: cold fluid

III. DATA REDUCTION AND GOVERNING EQUATIONS

The heat transfer rate was calculated based on the temperature difference and flow characteristics. The heat transfer coefficient was determined as follows:

The heat transfer rate is calculated using:

$$Q = \dot{m}\, Cp\, (Tout - Tin)$$

The heat transfer coefficient is given by:

$$h = Q / (A\, \Delta Tlm)$$

The Nusselt number is calculated as:

$$Nu = hD / k$$

The performance evaluation criterion (PEC) is evaluated using:

$$PEC = (Nu / Nu_0) / (f / f_0)^{(1/3)}$$

Where the subscript "0" refers to the baseline heat exchanger configuration without twisted tape inserts.

IV. RESULTS AND DISCUSSION

The numerical examination of STHXs is carried out using ANSYS Fluent R24/25 with varied fluid mass flow rates at the tube side ranging from 0.23 to 0.43 kg/s. It is evaluated using thermohydraulic metrics such as the heat transfer coefficient, Nusselt number, thermal efficiency, performance assessment criteria, pressure drop, and friction factor.

➢ *Influence of Mass Flow Rate on Heat Transfer Performance*

The relationship between the Nusselt number and heat transfer coefficient (HTC) and mass flow rate for different twisted tape pitches is shown in Figures 5 and 6. A greater mass flow rate causes a higher Reynolds number and increased turbulence intensity, which increases convective heat transfer by encouraging better fluid mixing and decreasing thermal boundary layer thicknesses. Among the configurations examined, the twisted tape with a 150 mm pitch had the greatest average Nusselt number due to optimum swirl formation, stronger secondary flow, and improved fluid mixing. The Nusselt number augmentation relative to the baseline configuration is found to be 10.84%, 17.55%, 23.52%, and 31.21% for twisted tape pitches of 50, 100, 200, and 150 mm, respectively.

ISSN No: -2456-2165 https://doi.org/10.38124/ijisrt/26apr2362

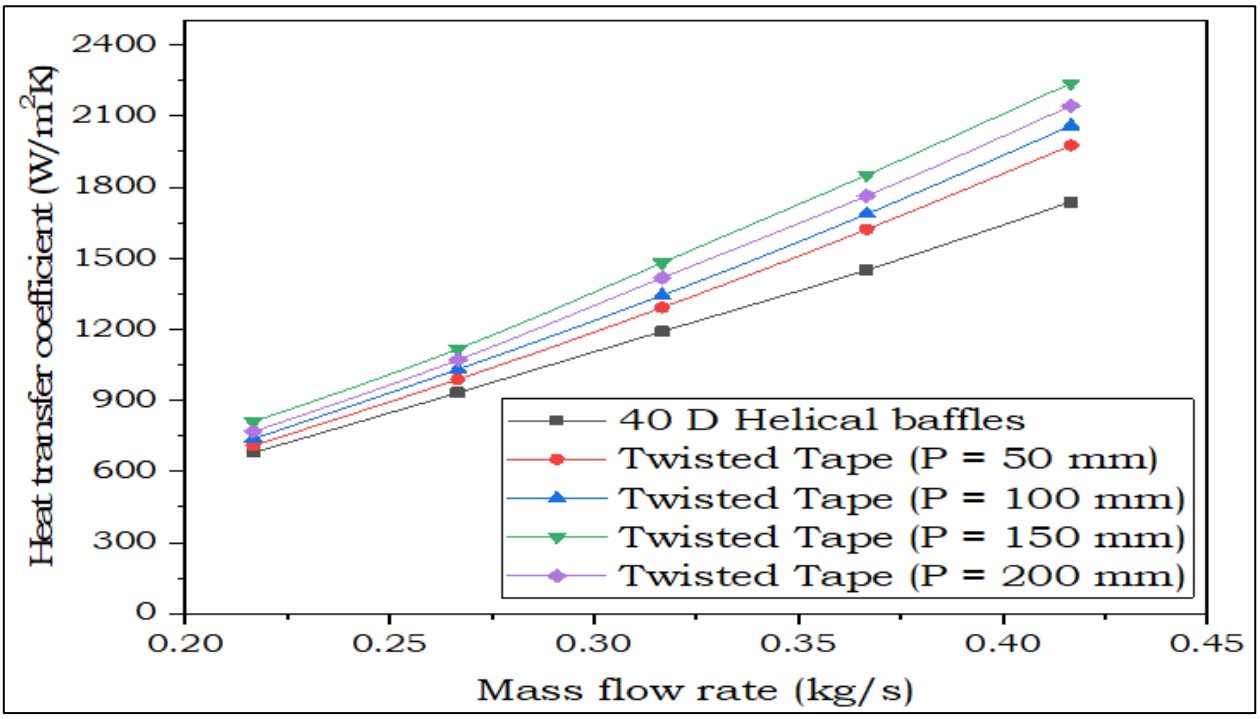

Fig 5 HTC vs Mass Flow Rate

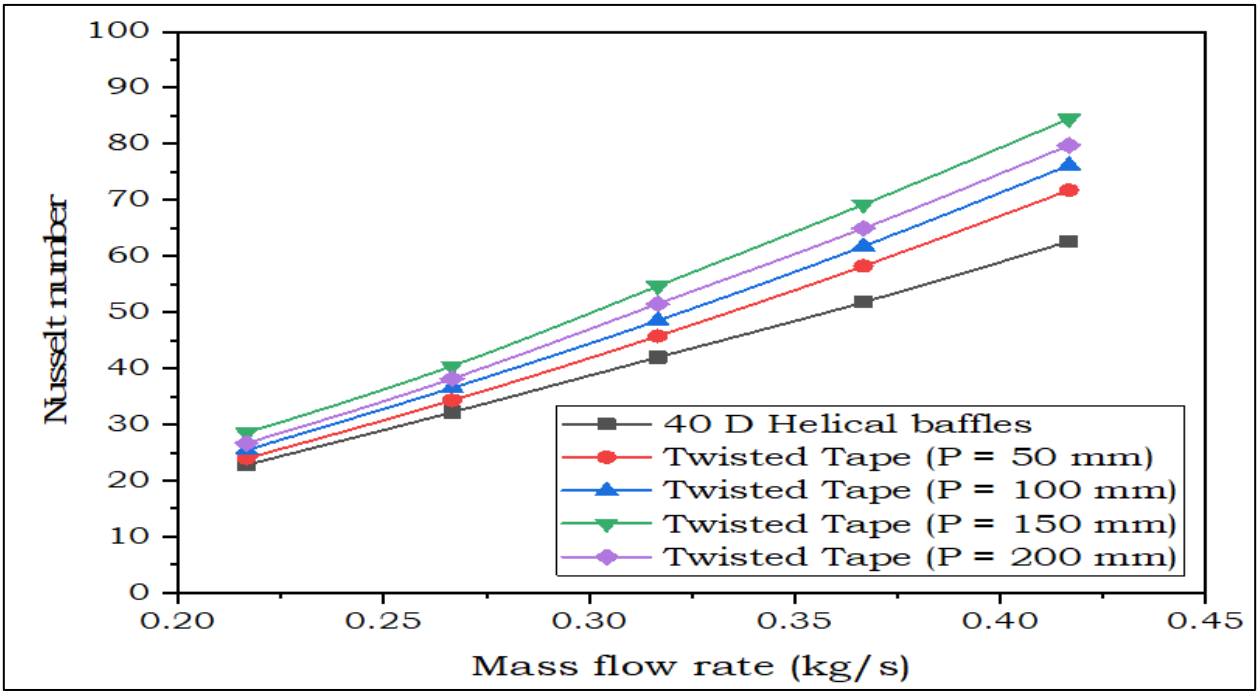

Fig 6 Nu vs Mass Flow Rate

➢ *Thermal Performance and Performance Evaluation Criterion*

Figure 7 depicts the relationship between thermal performance (TP) and performance evaluation criterion (PEC) and tube-side mass flow rate for various twisted tape pitches. As the mass flow rate increases, the thermal performance drops at first and then increases. This tendency is ascribed to the combined effects of increased convective heat transfer caused by swirl flow and the resulting rise in flow resistance. Among the configurations tested, the twisted tape with a pitch of 150 mm had the best thermal performance, showing a more effective heat transfer enhancement than other pitch values. When compared to the helical baffle arrangement, thermal performance improves by 8.54%, 10.62%, 18.23%, and 14.60% for twisted tape pitches of 50, 100, 150, and 200 mm, respectively.

Figure 8; Variation of Thermal Performance and Evaluation Criteria with Mass Flow Rate. The fluctuation of the performance evaluation criterion (PEC) with mass flow rate follows a similar trend. The PEC first drops at lower mass flow rates owing to hydraulic losses, but then increases

ISSN No: -2456-2165 https://doi.org/10.38124/ijisrt/26apr2362

at higher mass flow rates when heat transfer enhancement becomes more substantial. The highest PEC is achieved with a twisted tape pitch of 150 mm, indicating an appropriate compromise between heat transfer improvement and hydraulic penalty. Under the tested operating circumstances, the PEC increases by 1.55%, 10.84%, and 8.71% in comparison to the helical baffle arrangement.

➢ *Pressure Drop and Friction Factor*

Figure 9 and 10 shows how the tube-side pressure drop and friction factor change as the mass flow rate increases. Because of increased flow resistance and turbulence intensity, both metrics rise as the mass flow rate increases. The lowest pressure drop and friction factor are obtained at twisted tape pitches of 200 mm. However, compared to larger pitch values, a pitch of 150 mm offers the highest overall thermo-hydraulic performance because of increased swirl flow and more efficient disruption of the thermal boundary layer. The observed patterns are similar with earlier research described in the literature, indicating that the experimental results are reliable.

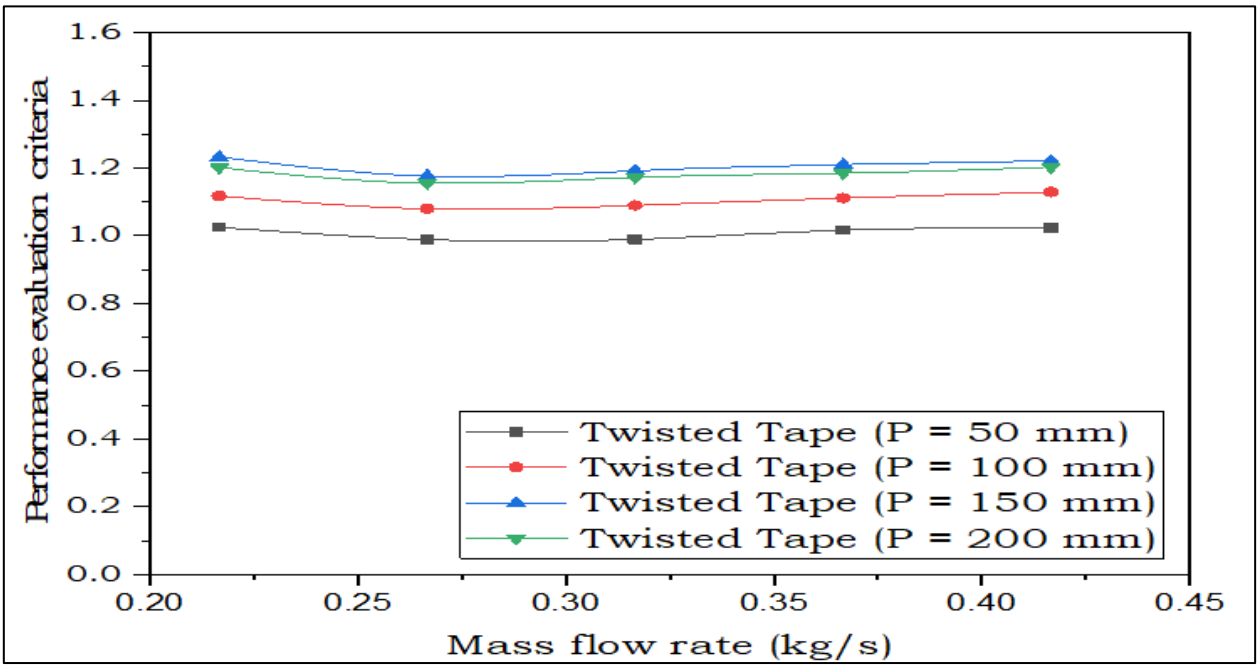

Fig 7 PEC vs Mass Flow Rate

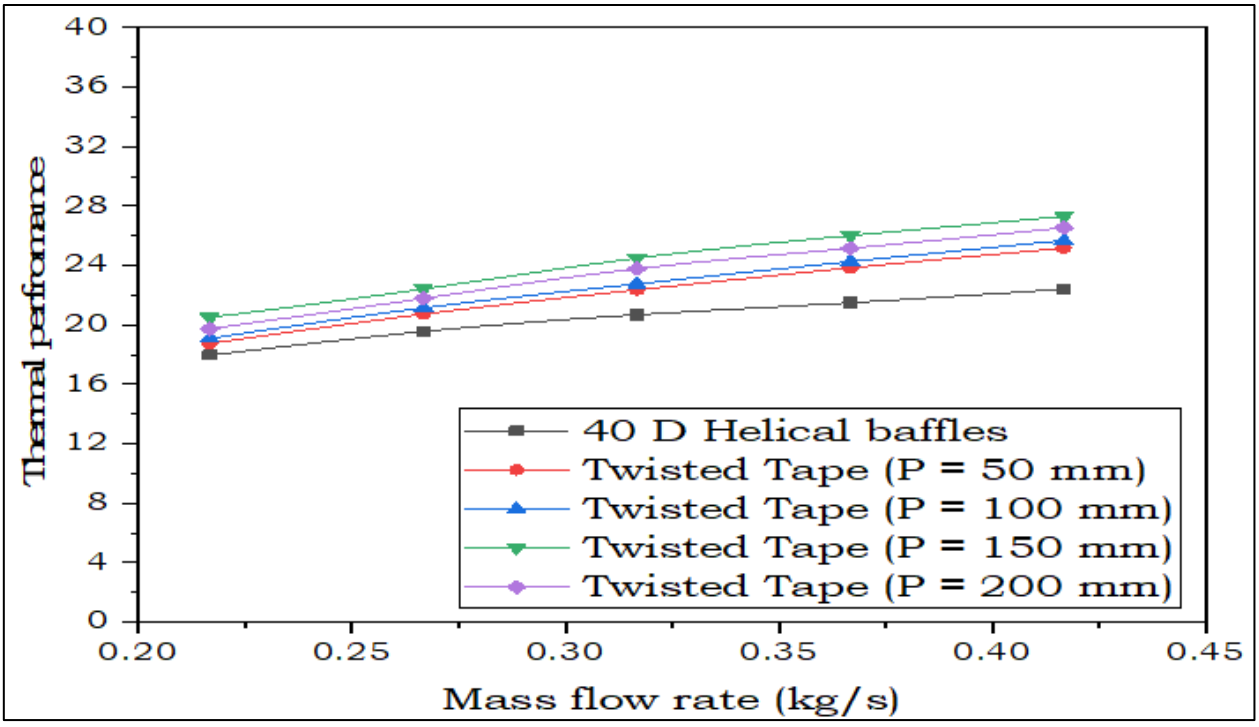

Fig 8 Thermal Performance vs Mass Flow Rate

ISSN No: -2456-2165 https://doi.org/10.38124/ijisrt/26apr2362

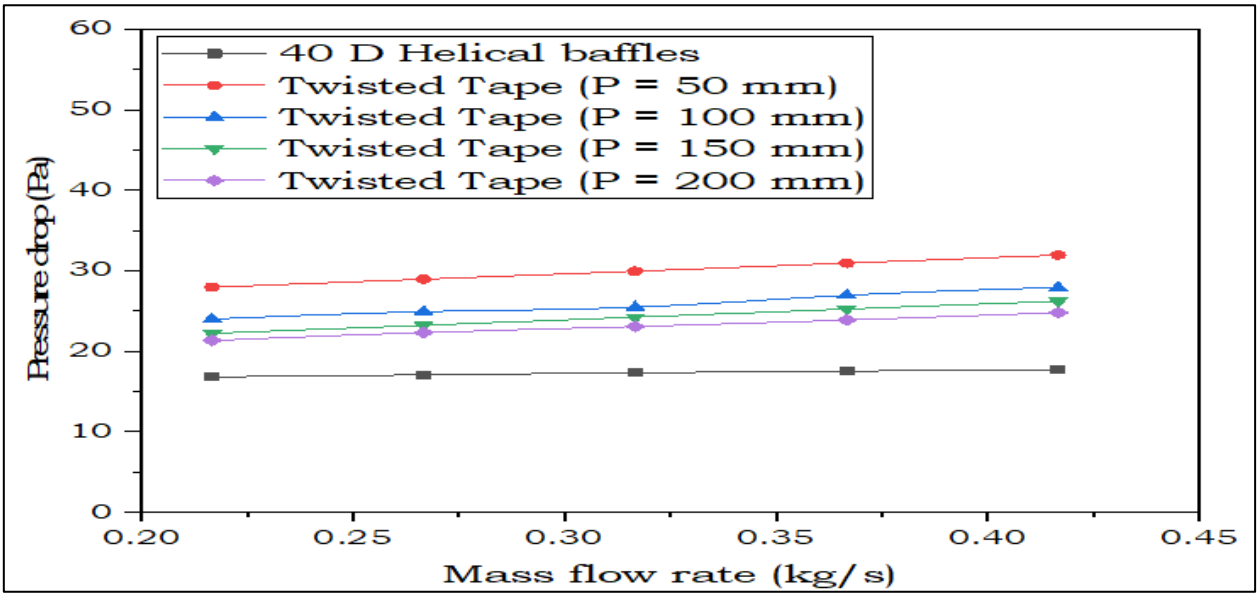

Fig 9 Pressure Drop vs Mass Flow Rate

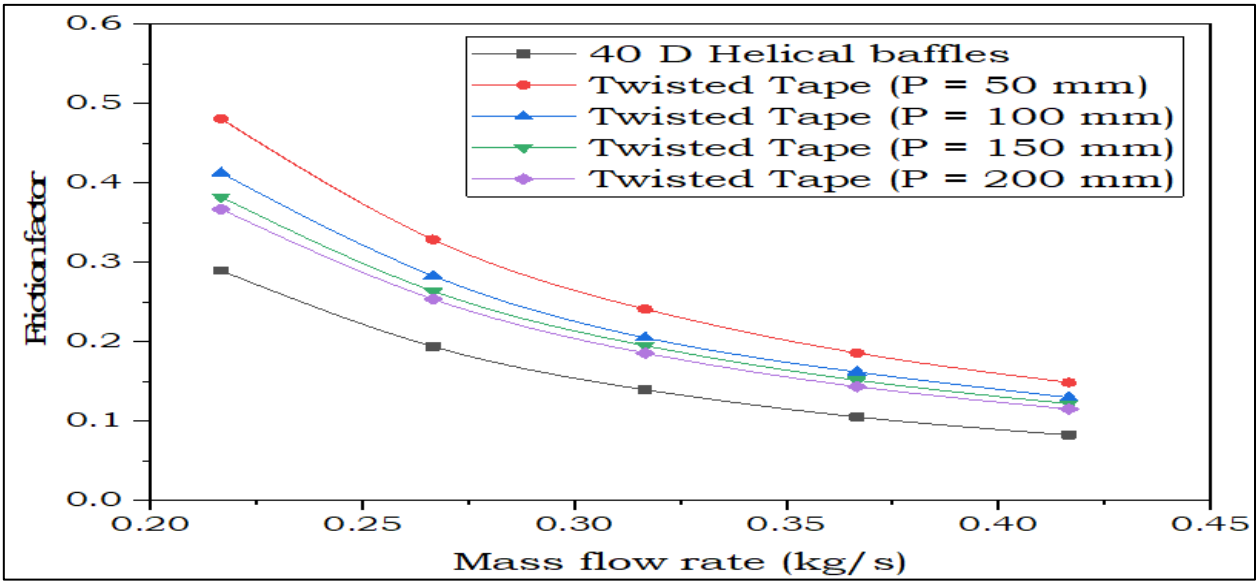

Fig 10 Friction Factor vs Mass Flow Rate

V. CONCLUSIONS

The thermohydraulic performance of a shell-and-tube heat exchanger with helical baffles and twisted tape inserts is evaluated using numerical simulation. The following findings have been reached:

- Twisted tape inserts improve tube-side heat transmission by creating swirl flow and increased turbulence intensity.
- At 150 mm twisted tape pitch, the Nusselt number increases by up to 31.21% relative to the baseline design.
- Using twisted tape inserts increases pressure loss, but the hydraulic penalty stays within acceptable ranges.
- According to performance evaluation criteria, a twisted tape pitch of 150 mm yields the best thermo-hydraulic performance.
- The combined influence of helical baffles and twisted tape inserts on enhancement of heat transfer in shell and tube heat exchanger is superior than the others.

- *Nomenclature:*

Table 1 Nomenclature

Symbol	Description	Unit
(A)	Heat transfer area	m^2
(C_p)	Specific heat capacity	$J \cdot kg^{-1} \cdot K^{-1}$
(D)	Inner diameter of tube	m

ISSN No: -2456-2165 https://doi.org/10.38124/ijisrt/26apr2362

(f)	Friction factor	–
(h)	Convective heat transfer coefficient	$W \cdot m^{-2} \cdot K^{-1}$
(k)	Thermal conductivity of fluid	$W \cdot m^{-1} \cdot K^{-1}$
(\dot{m})	Mass flow rate	$kg \cdot s^{-1}$
(Nu)	Nusselt number	–
PEC	Performance evaluation criterion	–
(Q)	Heat transfer rate	W
(Re)	Reynolds number	–
(T_{in})	Inlet temperature	K
(T_{out})	Outlet temperature	K
(\Delta T_{lm})	Log mean temperature difference	K

REFERENCES

[1]. Chen, J., Ling, Z., Fang, X., Wu, Y., & Zhang, Z. (2025). Numerical simulation on the flow and heat transfer characteristics of molten salt nanofluid in the shell-side of helical baffle heat exchangers with elliptic tubes and circular tubes. Solar Energy Materials and Solar Cells, 290, 113733.

[2]. Dinesh Babu, C., Shiva Sankaran, N., Raja, K. V., & Venkatesh, R. (2024). Performance analysis of baffle configuration effect on thermo-hydraulic behaviour of shell and tube heat exchanger. Journal of Thermal Analysis and Calorimetry, 149(12), 6253-6264.

[3]. Saad, M., Munir, A., & Kamran, M. A. (2023). Numerical simulations of shell and tube heat exchanger with segmental, trefoil and segmented trefoil baffles for performance comparison. Heat Transfer Engineering, 44(8), 702-719.

[4]. Gugulothu, R., & Sanke, N. (2022). Effect of helical baffles and water-based Al_2O_3, CuO and SiO_2 nanoparticles in the enhancement of thermal performance for shell and tube heat exchanger. International Journal of Heat Transfer, 1–26.

[5]. Cao, K., Liang, J., Ma, W., Tan, Z., Kang, Z., Huang, S., & Li, L. (2025). Performance optimization of Y-shaped helical baffle heat exchangers using response surface methodology. Applied Thermal Engineering, 127002.

[6]. Cheng, L., Liu, Z., Gu, H., Wu, J., Chen, Y., & Sunden, B. (2025). Recent advances of helical baffle heat exchangers: Principles, structural optimization, application and beyond. Applied Thermal Engineering, 126390.

[7]. Shuai, Z., Lei, X., Ge, D., Shen, Y., Zhang, J., Guo, R., ... & Wang, Y. (2025). Thermal performance of condensation phase change in the shell side of discontinuous helical baffle heat exchanger. Case Studies in Thermal Engineering, 68, 105959.

[8]. Lu, G., Sun, L., Zhao, C., Zhang, X., Si, W., & Luan, D. (2024). Flow Characteristics and Heat Transfer Performances of Quadrant Helical Baffle Heat Exchanger with Grooved Joint. Heat Transfer Engineering, 45(14), 1247-1256.

[9]. Cheng, J., Cheng, W., Lin, W., & Yu, J. (2024). Heat Transfer Performance and Flow Characteristics of Helical Baffle–Corrugated Tube Heat Exchanger. Applied Sciences, 14(19), 8905.

[10]. Vivek, S., Vishnu, V., Dipin, K. R., & Jithu, J. (2024). Continuous helical baffle heat exchanger: an experimental investigation. In Challenges and Opportunities in Industrial and Mechanical Engineering: A Progressive Research Outlook (pp. 246-254). CRC Press.

[11]. Kaleru, A., Venkatesh, S., & Kumar, N. (2022). Theoretical and numerical study of a shell and tube heat exchanger using 22% cut segmental baffle. *Heat Transfer*, 1–17

[12]. Hu, B., Liu, H., & Jin, M. (2023, September). Numerical simulation of thermo-hydraulic behaviour of shell and tube heat exchanger equipped with segmental baffle and helical baffle. In Journal of Physics: Conference Series (Vol. 2584, No. 1, p. 012050). IOP Publishing.

[13]. Gu, X., Shi, Q., Gao, W., Li, M., & Wang, D. (2023). Performance analysis and structural optimization of torsional flow heat exchangers with sinusoidal corrugated baffle. Journal of Thermal Science, 32(2), 680-691.

[14]. Jalili, P., Kazerani, K., Jalili, B., & Ganji, D. D. (2022). Investigation of thermal analysis and pressure drop in non-continuous helical baffle with different helix angles and hybrid nano-particles. Case Studies in Thermal Engineering, 36, 102209.

[15]. Marzouk, S. A., Abou Al-Sood, M. M., El-Fakharany, M. K., & El-Said, E. M. (2022). A comparative numerical study of shell and multi-tube heat exchanger performance with different baffles configurations. International Journal of Thermal Sciences, 179, 107655.

[16]. Chen, D., Zhang, R., Cao, X., Chen, L., & Fan, X. (2021). Numerical investigation on performance improvement of latent heat exchanger with sextant helical baffles. International Journal of Heat and Mass Transfer, 178, 121606.

[17]. Uosofvand, H., & Abbasian Arani, A. A. (2021). Shell-and-tube heat exchangers performance improvement employing hybrid segmental–helical baffles and ribbed tubes combination. Journal of the Brazilian Society of Mechanical Sciences and Engineering, 43(8), 399.

[18]. Gugulothu, R., Sanke, N., Nagadesi, S., & Jilugu, R. K. (2021, February). Thermal hydraulic performance of helical baffle shell and tube heat exchanger using RSM method. In International Conference on Applied Analysis, Computation and Mathematical Modelling

ISSN No: -2456-2165 https://doi.org/10.38124/ijisrt/26apr2362

in Engineering (pp. 167-187). Singapore: Springer Nature Singapore.
[19]. Wang, K., Liu, J. Q., Liu, Z. C., Chen, W., Li, X. C., & Zhang, L. (2021). Fluid flow and heat transfer characteristics investigation in the shell side of the branch baffle heat exchanger. Journal of Applied Fluid Mechanics, 14(6), 1775-1786.
[20]. Cao, X., Chen, D., Du, T., Liu, Z., & Ji, S. (2020). Numerical investigation and experimental validation of thermo-hydraulic and thermodynamic performances of helical baffle heat exchangers with different baffle configurations. International Journal of Heat and Mass Transfer, 160, 120181.
[21]. Abdelkader, B. A., Jamil, M. A., & Zubair, S. M. (2020). Thermal-hydraulic characteristics of helical baffle shell-and-tube heat exchangers. Heat Transfer Engineering, 41(13), 1143-1155.
[22]. Anbu, S., Arunkumar, P., Kamatchi, R., & Chellappan, M. (2025). Investigation of convective heat transfer in helically corrugated tubes with inserts using nanofluids. Journal of Thermal Analysis and Calorimetry, 1-18.
[23]. Marzouk, S. A., Sharaf, M. A., Aljabr, A., Almehmadi, F. A., Alam, T., & Malik, I. (2024). Effects of baffles and springs in shell and multi-tube heat exchangers: comparative approach. Case Studies in Thermal Engineering, 61, 104996.
[24]. Louahdi, M., Salhi, J. E., Essaouini, H., Zarrouk, T., & Lahlaouti, M. L. (2024). Three-dimensional analysis for optimizing thermo-hydrodynamic performance of heat exchangers with perforated semi-circular inserts. Case Studies in Thermal Engineering, 60, 104611.
[25]. Deshmukh, V., & Sarviya, R. M. (2024). Categorical review of experimental and numerical studies on twist tape inserts in the single-phase flow tubular heat exchanger. Journal of Thermal Analysis and Calorimetry, 149(7), 2985-3025.
[26]. Marzouk, S. A., Abou Al-Sood, M. M., El-Said, E. M., Younes, M. M., & El-Fakharany, M. K. (2023). A comprehensive review of methods of heat transfer enhancement in shell and tube heat exchangers. Journal of Thermal Analysis and 22Calorimetry, 148(15), 7539-7578.
[27]. Kaushik, S., Singh, S., & Panwar, K. (2023). Experimental study of fluid flow properties in spiral tube heat exchanger with varying insert shape over spiral tube profile. Materials Today: Proceedings, 80, 78-84.
[28]. Ifraj, N. F., Fahad, M. K., Tahsin, S. H., Haque, M. R., & Haque, M. M. (2023). Numerical investigation of the thermal performance optimization inside a heat exchanger tube using different novel combination of perforations on Y-shaped insert. International Journal of Thermal Sciences, 194, 108583.
[29]. Tavousi, E., Perera, N., Flynn, D., & Hasan, R. (2023). Heat transfer and fluid flow characteristics of the passive method in double tube heat exchangers: a critical review. International Journal of Thermofluids, 17, 100282.
[30]. Toygun Dagdevir, Mahmut Uyanik, and Veysel Ozceyhan. The experimental thermal and hydraulic performance analyses for the location of perforations and dimples on the twisted tapes in twisted tape inserted tube. International Journal of Thermal Sciences, Vol.: 167, 2021, 107033.
[31]. Marzouk, S. A., Abou Al-Sood, M. M., El-Fakharany, M. K., & El-Said, E. M. (2022). A comparative numerical study of shell and multi-tube heat exchanger performance with different baffles configurations. International Journal of Thermal Sciences, 179, 107655.
[32]. Pongjet Promvonge, Narin Koolnapadol, Monsak Pimsarn, and Chinaruk Thianpong. Thermal performance enhancement in a heat exchanger tube fitted with inclined vortex rings. Applied Thermal Engineering, Vol.: 62, 2014, pp: 285-292.
[33]. Suabsakul Gururatana and Sompol Skullong. Heat transfer augmentation in a pipe with 3D printed wavy insert. Case Studies in Thermal Engineering, Vol.: 21, 2020, 100698.
[34]. Cheng, L., Liu, Z., Gu, H., Wu, J., Chen, Y., & Sunden, B. (2025). Recent advances of helical baffle heat exchangers: Principles, structural optimization, application and beyond. Applied Thermal Engineering, 126390.
[35]. Waleed, M., Naqvi, S. M. A., Mustafa, H., Al Mesfer, M. K., Danish, M., Irshad, K., & Shahzad, H. (2025). Numerical analysis of shell and tube heat exchanger with combination of different baffles. Case Studies in Thermal Engineering, 65, 105658.
[36]. Mohadjer, A., Nobakhti, M. H., Nezamabadi, A., & Ajarostaghi, S. S. M. (2024). Thermohydraulic analysis of nanofluid flow in tubular heat exchangers with multi-blade turbulators: The adverse effects. Heliyon, 10(9).
[37]. Leong K.Y, Saidur R, Kazi S.N., and Mamun A.H. Performance investigation of an automotive car radiator operated with nanofluid-based coolants (nanofluid as a coolant in a radiator). Applied Thermal Engineering, Vol.: 30, 2010, pp: 2685-2692.
[38]. Ramin Mashayekhi, Erfan Khodabandeh, Mehdi Bahiraei, Leyli Bahrami, Davood Toghraie, and Omid Ali Akbari. Application of a novel conical strip insert to improve the efficacy of water-Ag nanofluid for utilization in thermal systems: A two-phase simulation. Energy Conversion and Management, Vol.: 151, 2017, pp: 573-586.
[39]. Saleh B and Syam Sundar L. Experimental study on heat transfer, friction factor, entropy and exergy efficiency analyses of a corrugated plate heat exchanger using Ni/water nanofluids. International Journal of Thermal Sciences, Vol.: 165, 2021, pp: 106935.